# Polypropylene/glass fiber/nanoclay hybrid composites: morphological, thermal, dynamic mechanical and impact behaviors

Normasmira A Rahman, Aziz Hassan, R Yahya, RA Lafia-Araga and PR Hornsby

*Journal of Reinforced Plastics and Composites* 2012 31: 1247
DOI: 10.1177/0731684412456445

Article

JOURNAL OF REINFORCED PLASTICS & COMPOSITES

*Journal of Reinforced Plastics and Composites*
31(18) 1247–1257

DOI: 10.1177/0731684412456445
jrp.sagepub.com

SAGE

# Polypropylene/glass fiber/nanoclay hybrid composites: morphological, thermal, dynamic mechanical and impact behaviors

**Normasmira A Rahman[1], Aziz Hassan[1], R Yahya[1], RA Lafia-Araga[1,2] and PR Hornsby[3]**

**Abstract**

Polypropylene/E-glass fiber/nanoclay were compounded with a twin-screw extruder and injection molded. Thermal, dynamic mechanical, and impact tests were carried out. Differential scanning calorimetry investigations showed that the incorporation of nanoclay into polypropylene/glass fiber composite shifted the melting temperature ($T_m$) to higher values. The degree of crystallinity ($X_c$) was strongly influenced by the presence of the glass fiber and nanoclay in the matrix. Dynamic mechanical analysis showed an increase in storage modulus ($E'$); indicating higher stiffness of the hybrid composites when compared to the glass fiber composites and the virgin matrix. From the tan $\delta$ curves, a strong influence of glass fiber and nanoclay content on the magnitude of tan $\delta_{max}$ value was observed. Impact test showed a reduction in the critical strain energy release rate, $G_c$ for hybrid composites with higher nanoclay loading. The stress intensity factor, $K_c$ values showed insignificant effect with the presence of nanoclay and GF.

**Keywords**

Mechanical characterization, composites, nanostructured materials, fracture, nucleation

## Introduction

Fiber-reinforced plastic (FRP) composites, with a wide variety of matrix polymers, have been developed as an alternative to thermoset fiber composites. Because of its well-balanced physical and mechanical properties, the relative ease of processing and its relative low cost,[1] polypropylene (PP), a semi-crystalline engineering thermoplastic) has many potential applications in the automotive and commercial products. Glass fiber (GF) reinforced polymers have been widely used in the automotive and aerospace industries because of their high strength and low-weight characteristics. However, due to high stress concentration and poor fiber-matrix adhesion, it has been shown, that incorporation of short GF (SGF) in PP increases the tensile modulus, yet decrease the tensile strength and impact toughness.[2] By contrast, Karger-Kocsis[3] conducted a study on the dependence of the fracture and fatigue performance of polyolefins, related blends, and composites on their microstructural and molecular characteristics. The author reported that the fracture toughness and resistance of the related composites increases with increasing crystallinity up to a maximum, if other parameters such as lamellar thickness, orientation, amorphous layer, and tie molecules are constant.

Polymer nanocomposites based on exfoliated nanoparticles are a different type of composite material. They contain extremely small particles, with thickness in the range of 1 nm. In general, nanoparticles can significantly improve the stiffness, heat deflection temperature, dimensional stability, gas barrier properties,

[1]Department of Chemistry, University of Malaya, Kuala Lumpur, Malaysia
[2]Department of Chemistry, Federal University of Technology, Minna, Nigeria
[3]School of Mechanical and Aerospace Engineering, Queen's University Belfast, Belfast, United Kingdom

**Corresponding author:**
Aziz Hassan, Department of Chemistry, University of Malaya, 50603 Kuala Lumpur, Malaysia.
Email: ahassan@um.edu.my

electrical conductivity, and flame retardancy of the polymer matrix.[4]

Recently, it has been observed[5–8] that by incorporating nanoparticles into the matrix of fiber-reinforced composites (hybrid), synergistic effect may be achieved. Hybrid composites are those composites which have a combination of two or more reinforcement fibers in a pre-determined geometry and scale; making them suitable to serve specific engineering purpose. The length scale of the property improvement in the FRP composites and nanocomposites are very different. For example, the thickness of an exfoliated silicate sheet is 10,000 times smaller than that of the diameter of a typical GF. Therefore, the two materials can be combined in a new type of a three-phase hybrid composite. In this new composite system, the main reinforcing phase is the discontinuous fibers. The matrix itself is supposedly a composite too, containing particles on the nanometer length scale. A schematic drawing of this concept has been explained by Vlasveld et al.[9] The particles in the matrix material fit between the fibers, without reducing the fiber volume fraction. The matrix-dominated properties of the fiber composite can benefit from the improved properties imparted by the nanoparticles.

These hybrid composites often exhibit remarkable improvement in materials properties when compared with the conventional micro- and macro-composites.[10] It has been observed that by incorporating filler particles into the matrix of fiber-reinforced composites, synergistic effects can be achieved in the form of reduction in material costs, increased modulus, heat resistance and biodegradability (of biodegradable polymers), decrease gas permeability, and flammability. However, due to stress concentration, agglomeration, and confinement of matrix molecular mobility around the rigid filler phase, the impact toughness is reduced.[11]

The most prominent effect of particulate fillers on the crystalline structure of semi-crystalline thermoplastics is their ability to work as nucleation agents. Though there has been some debate over the effects of crystalline changes on macro-mechanical properties, it seems clear that upon increasing crystallinity, the modulus of PP increases, while the mechanical strength and deformability decrease.[12] The effectiveness of nanoclay (NC) on improving properties of hybrid composite strongly depends on the size, shape, aspect ratio, interfacial adhesion, surface characteristics, and the degree of dispersion.[13]

However, hybrid-reinforced composites form a complex system and there is inadequate data available about the phenomena behind the property changes due to the addition of particulate fillers to the fiber-reinforced thermoplastic composites. Thus, this article is an attempt to clarify the thermal, dynamic mechanical, and impact behaviors of hybrid composites based on: PP matrix, SGF reinforcement, and NC particulate filler. PP/clay nanocomposite systems were prepared for use as a matrix material for GF composites. An experimental study was carried out to exploit the functional advantages and potentially synergistic effect of GF and NC, in order to enhance the overall properties of PP. As a comparison, the properties of PP/GF composite and PP/NC nanocomposite were also evaluated under identical test conditions. The structures of PP/NC and PP/GF/NC were investigated using the transmission electron microscopy (TEM) and the scanning electron microscopy (SEM). Thermal, dynamic mechanical and, impact properties of the composites were also investigated by differential scanning calorimetry (DSC), dynamic mechanical analysis (DMA), and impact test, respectively.

## Experimental

### Materials

PP (Propelinas H022) was supplied by Petronas, Malaysia. The neat PP was in the form of pellets with a melt flow index of 11 g/10 min (at 230°C, load 2.16 kg) and a density of 910 kg/m$^3$. Chopped E-GF, surface-treated with silane and having a density of 2550 kg/m$^3$, average diameter of 14 μm, and length of 6 mm, obtained from KCC Corporation, Korea and used as the principle reinforcement. The NC (type PGV), is a natural untreated montmorillonite clay, with a density of 776 kg/m$^3$ and a particle size of about 16 μm and manufactured by Nanocor, USA.

### Specimen preparation

PP/GF and PP/NC composites were prepared with different ratios of PP/GF and PP/clay powder, as presented in Table 1. Compositions were physically premixed and then compounded using the Brabender, KETSE 20/40 (Germany) twin-screw extruder with the screw diameter and screw aspect ratio of 20 mm and 40, respectively. The temperature profile was set between 185°C and 190°C. For the PP/GF composites, the screw speed was set to 100 rpm, whereas for the PP/NC composites, the screw speed used was 800 rpm. The materials extruded from both formulations were pelletized into length of about 6 mm. In order to produce PP/GF/NC composites, the different ratios of the PP/NC and GF were physically mixed and re-compounded in a twin-screw extruder, using the same temperature profile and screw speed of 100 rpm. The dumb bell-shaped tensile and impact tests specimens, according to ASTM standard D638[14] and ASTM Standard E23,[15] respectively, were then injection molded using a Boy® 55 M (Germany), with a 55 ton clamping force

**Table 1.** Designation and compositions of composite specimens

| Sample | Matrix weight fraction, $W_m$ (%) | Fiber weight fraction, $W_f$ (%) | Fiber volume fraction, $V_f$ (%) | Clay content (phr)[a] |
|---|---|---|---|---|
| NC (clay) | – | – | – | – |
| PP | 100 | – | – | – |
| PP85/G15 | 85 | 15 | 6 | – |
| PP100/NC3 | 100 | – | – | 3 |
| PP100/NC6 | 100 | – | – | 6 |
| PP100/NC9 | 100 | – | – | 9 |
| (PP85/G15)/NC3 | 85 | 15 | 6 | 3 |
| (PP85/G15)/NC6 | 85 | 15 | 6 | 6 |
| (PP85/G15)/NC9 | 85 | 15 | 6 | 9 |

PP: polypropylene; NC: nanoclay.
[a]phr = parts per hundred parts of resin.

injection molding machine. The processing temperature was set between 175°C and 185°C and the mold temperature was set at 25°C. The screw speed was maintained at 30–50 rpm. The list and abbreviation of specimens prepared are given in Table 1.

### *Microstructural characterization*

The microstructure of the PP/NC and PP/GF/NC were analyzed with a Hitachi H-600 (Japan) TEM. The samples were ultramicrotomed with a diamond knife on a Leica Ultracut UCT (UK) microtome at room temperature to give section with a nominal thickness of 200 nm. Sections were transferred to 400 mesh Cu grids. Bright-field TEM images of the composites were obtained at an acceleration voltage of 300 keV.

The fracture surface of the various nanocomposites was examined using a JEOL Field Emission Auger Microprobe model JAMP-9500F (Japan) under SEM mode, to investigate the effects of clay loading on the adhesion at the interface between GF and the PP matrix and the extent of clay dispersion. SEM micrographs were taken at 10 keV accelerating voltage at various magnifications. The fracture surface of tensile specimens was sputter-coated with a thin layer of gold to improve the sample conductivity and to avoid electrical charging during examination.

### *Differential scanning calorimetry*

DSC experiments were performed with a Perkin Elmer Diamond DSC (USA). Each sample was subjected to heating and cooling cycles at a scanning rate of 10°C/min under nitrogen atmosphere with the nitrogen flow rate of 20 mL/min, in order to prevent oxidation. The test sample of between 5 and 10 mg was crimped in an aluminum pan and tested over a temperature range of 0°C–190°C.

### *Determination of dynamic mechanical properties*

The dynamic mechanical properties of specimens were analyzed with a Thermal Analysis Instrument, TAI Q800 (USA) DMA. Test specimens were taken from the mid-section of the injection molded dumb-bell test bar and were subjected to a three-point bending (3-PB) mode with a support span of 50 mm. Measurements were conducted over a temperature range of −100°C to 110°C with a heating rate of 3°C/min at a constant frequency of 1.0 Hz

### *Determination of impact properties*

The impact test bars of 60 mm × 12 mm × 6 mm (length × depth × width) dimensions were notched at the center of one edge to produce single-edge-notch (SEN) impact test specimen. The notch angle was set at 45°. Each batch was notched with four different notch-to-depth ($a/D$) ratios of 0.1, 0.2, 0.3, and 0.4. The support span-to-depth ratio ($S/D$) was maintained at 4 throughout the experiment. For each batch, a minimum of 12 specimens were tested and the results presented were taken from the average of at least eight reproducible data. The impact test was run under charpy mode using an Instron Dynatup 9210 (USA) instrumented falling weight impact tester with a V-shaped impactor tup. The test was carried out at 25°C, with fixed impactor weight (m) of 6.448 kg, impactor velocity (v) of 0.9238 m/s, and impact energy of 2.7512 J. ASTM standard E23 was used as a standard in calculating the impact properties.[15]

## Results and discussion

### *Transmission electron microscopy*

To gain an insight into the morphology of the nanocomposites, characterization using TEM was conducted at low and high magnifications for 3, 6, and 9 phr NC-based nanocomposite samples, as shown in Figure 1. Nanocomposites containing 3–9 phr of NC show heterogeneous dispersion, presence of aggregates, as well as resin-rich areas in the matrix without clay. However, there are regions where completely delaminated sheets are dispersed individually, showing as average dark lines of 1–2 nm thickness. It appears as if the clay exists as expanded aggregates. The size of the aggregates and the number of platelets in the composites increase with the percentage of clay within the

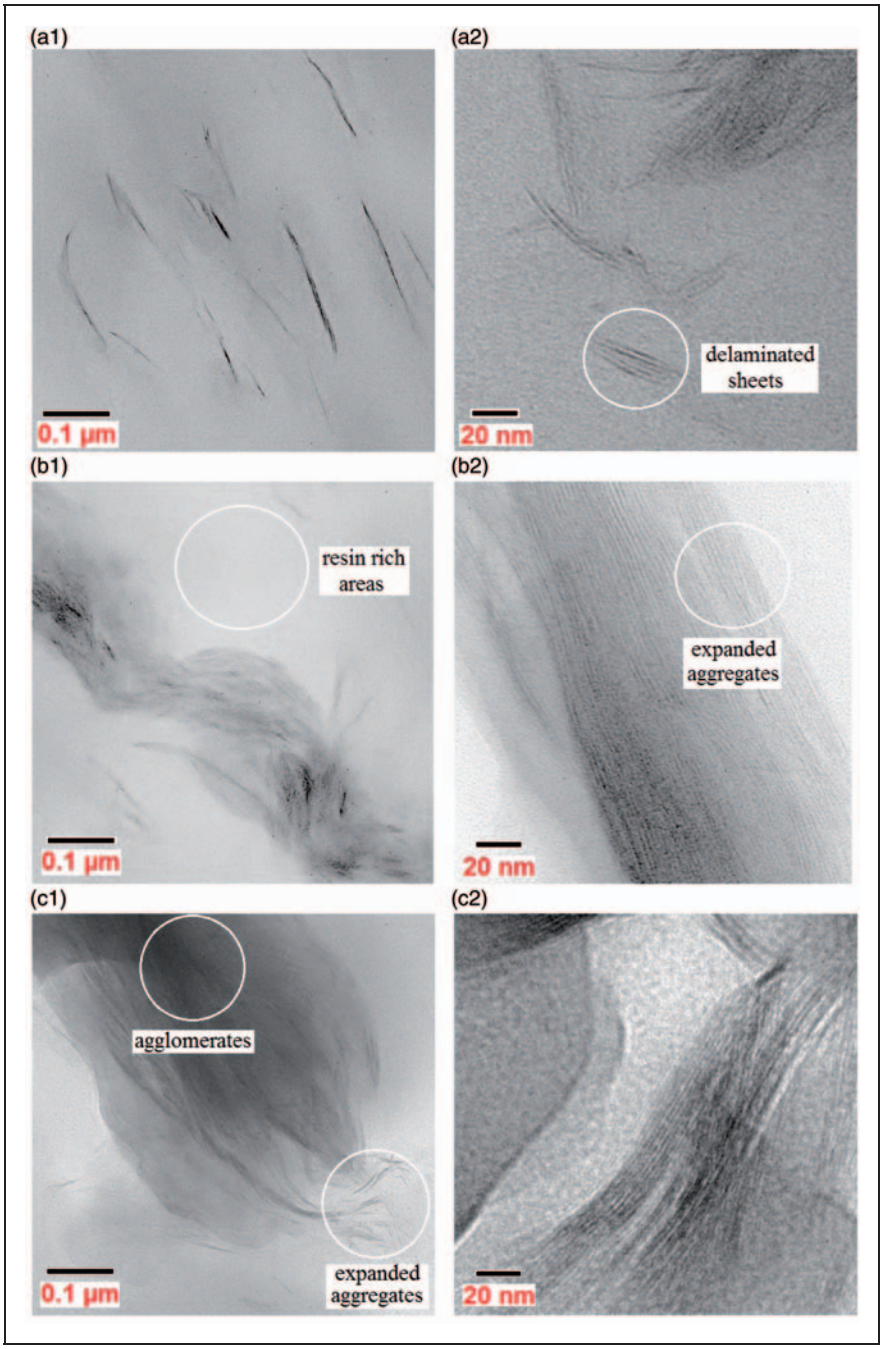


**Figure 1.** TEM images of PP/NC as a function of NC concentration: (a1) and (a2) for PP/NC3; (b1) and (b2) for PP/NC6; (c1) and (c2) for PP/NC9; left side at low magnification (29,000×); right side at high magnification (97,000×).
TEM: transmission electron microscopy; PP: polypropylene; NC: nanoclay.

PP matrix. Hussain et al.[16] suggested that the degree of intercalation or exfoliation depends on the type and surface modification of NC, presence of compatibilizing agent, as well as the processing condition. Within the scope of this study, untreated NC has been used. Therefore, a homogeneous dispersion of layered silicates is difficult to attain as the NC has a strong tendency to agglomerate and interaction between PP and NC may be poor as no compatibilizer has been added.

It has been reported in our previous publication, that the interlayer spacing from X-ray diffraction characterization for NC in PP/NC3 composite is expanded when compared with the composites with higher NC

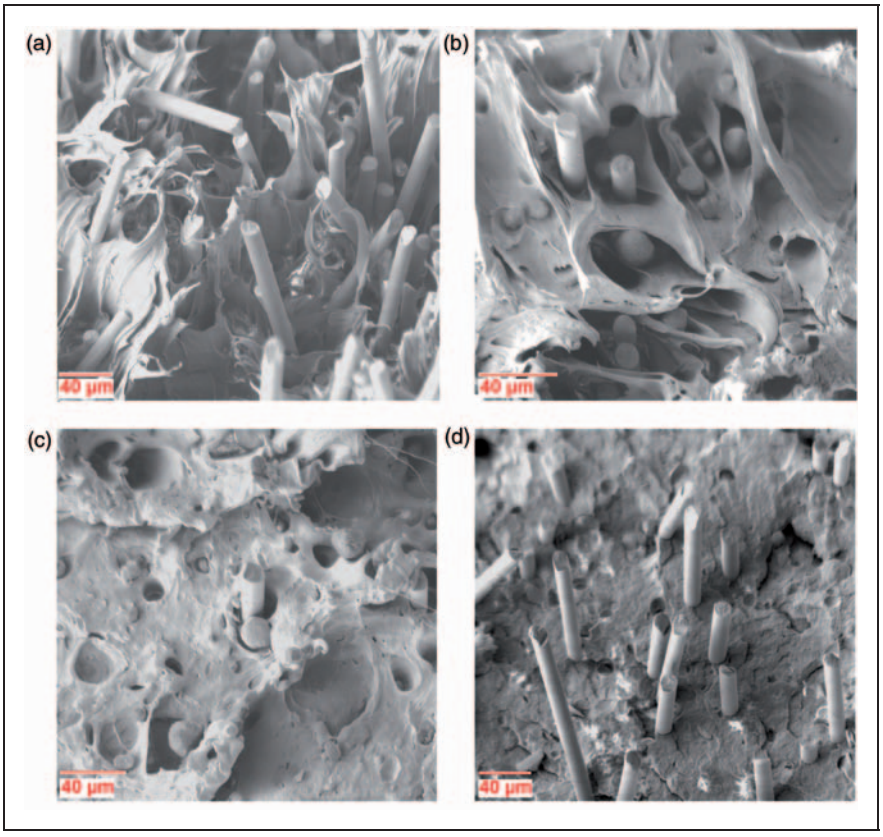


**Figure 2.** SEM micrographs of impact fractured surfaces of: (a) PP:G15; (b) (PP:G15)/NC3; (c) (PP:G15)/NC6; and (d) (PP:G15)/NC9.
SEM: scanning electron microscopy; PP: polypropylene; NC: nanoclay.

loading.[8] The PP/GF/NC hybrid composites were also examined by TEM, where structure and orientation of NC was unclear. The hybrid composites were therefore analyzed with SEM.

## *Scanning electron microscopy*

The impact fractured surfaces of 15 wt% GF composites with different amounts of NC, were studied by SEM (Figure 2). In the case of composite with 15 wt% GF without NC (Figure 2(a)), there is clear evidence of ductile matrix deformation, which is a result of the fiber debonding and pull-out processes. On the other hand, a more brittle fracture surface is observed in the case of the corresponding hybrid composites with NC contents of 3–9 phr (Figure 2(b) to (d)). It can be noted from Figure 2 that ductility is reduced with increase in NC content, as evidenced by the smaller deformation patterns when compared with PP/GF composite. It can be concluded that this ductility reduction of the matrix also contributes to the decrease in impact strength when NC is added to the PP/GF composite.[5] These SEM observations are in good agreement with the impact test result, which will be discussed later.

## *Differential scanning calorimetry*

The DSC thermograms allow one to get information on the melting temperature ($T_m$), crystallization temperature ($T_c$), enthalpy heat of melting ($\Delta H_m$), and the enthalpy heat of crystalline ($\Delta H_c$). The degree of crystallinity ($X_c$) of the specimens was calculated using equation (1)[2]

$$X_c(\%) = \frac{\Delta H_m}{\Delta H_m^*} \tag{1}$$

where $\Delta H_m^*$ is enthalpy heat of fusion of an 'ideally' fully crystalline PP, taken as 209 J/g.[10] The $\Delta H_m$, $\Delta H_c$, and $X_c$ values of PP, PP/GF, PP/NC, and PP/GF/NC have been normalized and computed according to the actual PP content in the composites, as seen in Table 2.

DSC thermograms show the presence of single peaks for the heating and cooling scans of the composites (Figures 3 and 4). The melting temperature of pure PP is 163°C. DSC thermograms from Figure 3 show

**Table 2.** DSC data of GF composites

| Sample | $T_m$ (°C) | $\Delta H_m$ (J/g) | $X_c$ (%) | $T_c$ (°C) | $\Delta H_c$ (J/g) |
|---|---|---|---|---|---|
| PP | 163.0 | 75.1 | 35.9 | 121.7 | 93.1 |
| (PP85:G15) | 161.6 | 71.7 | 34.3 | 121.7 | 91.9 |
| (PP100)/NC3 | 162.0 | 53.1 | 25.4 | 121.4 | 67.6 |
| (PP100)/NC6 | 163.5 | 67.9 | 32.5 | 121.6 | 93.2 |
| (PP100)/NC9 | 163.6 | 73.4 | 35.1 | 122.8 | 94.1 |
| (PP85:G15)/NC3 | 163.8 | 70.8 | 33.9 | 125.5 | 96.0 |
| (PP85:G15)/NC6 | 165.5 | 85.4 | 40.8 | 130.3 | 96.1 |
| (PP85:G15)/NC9 | 164.9 | 82.1 | 39.3 | 129.7 | 98.7 |

DSC: differential scanning calorimetry; PP: polypropylene; NC: nanoclay.

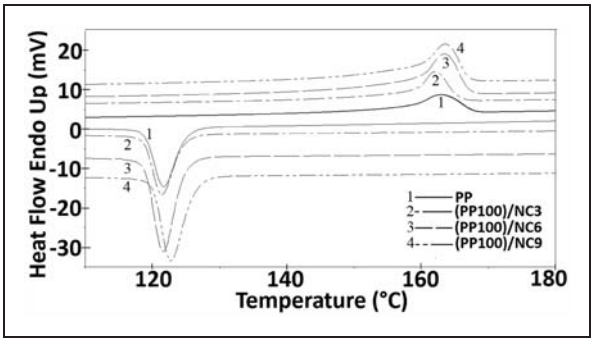


**Figure 3.** The DSC thermograms of injection-molded PP/NC composite.
DSC: differential scanning calorimetry; PP: polypropylene; NC: nanoclay.

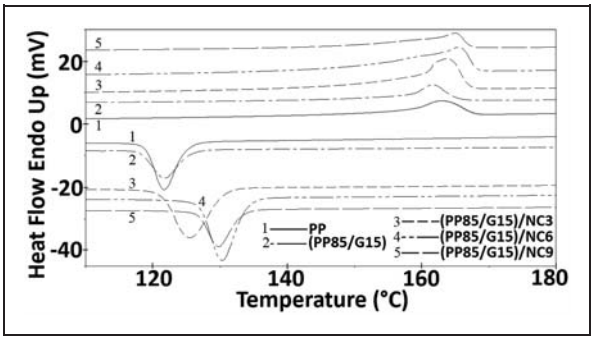


**Figure 4.** The DSC thermograms of injection-molded PP/GF/NC hybrid composites.
DSC: differential scanning calorimetry; PP: polypropylene; GF: glass fiber; NC: nanoclay.

that increasing the level of clay loading in PP/NC (PP/NC3-9) has insignificant effects on the melting temperature of the nanocomposites. Meanwhile, for PP/GF composite, incorporation of 15 wt% GF into the system slightly reduced the $T_m$ value (Figure 4 and Table 2). However, in the hybrid composites system, the $T_m$ value increased by about 2.5°C with increasing NC content. Among the composites studied, hybrid with 15 wt% GF and 6 phr NC ((PP:G15)/NC6) has the highest $T_m$ value of 165.5°C (Table 2 and Figure 4). Incorporation on GF and NC in PP seems to restrict the mobility of the polymer chain, resulting in higher $T_m$.

The $\Delta H_m$ is an important parameter since its magnitude is directly proportional to the overall level of $X_c$ possessed by the polymer.[17] The $\Delta H_m$ of unreinforced PP is 75.1 J/g and decreases to 71.7 J/g for the PP/G15 composite. Generally, the $\Delta H_m$ values for PP/NC nanocomposites are lower when compared with the neat PP. However, nanocomposite with higher clay content shows a higher $\Delta H_m$ value when compared with those with lower clay content. For the hybrid systems, it was observed that generally the $\Delta H_m$ values of composites increase with increasing clay content. The enthalpy heat of melting increases slightly with filler content of 6 phr, beyond which it decreases slightly. A slight reduction of $\Delta H_m$ was observed with the addition of 3 phr of clay into PP/GF15 composite. Further addition of 6 phr clay in the matrix, (PP/G15)/NC6 increases the $\Delta H_m$ to 85.4 J/g. However, composites, with 9 phr of clay, (PP/G15)/NC9 show a slight decrease in $\Delta H_m$ value.

For the PP/GF and PP/NC systems, introducing GF and NC interrupts the linear crystallizable sequence of the PP chains and lowers the degree of crystallinity,[18] indicating the fact that there is a large amount of the flexible amorphous content. Results from Table 2 show that the $X_c$ values of these composites are slightly reduced, relative to that of neat PP (35.9%). Meanwhile, for the hybrid composites, the addition of clay in the 15 wt% GF composite, shows some increment in the degree of crystallinity. An insignificant change (2.0% reduction) in $X_c$ was observed with the addition of 3 phr of clay to PP/GF15 composite, relative to PP. Further addition of 6 phr clay in the matrix, (PP:G15)/NC6 increases the $X_c$ value to 40.8%. It has been suggested that the presence of NC platelets dispersed in the GF composites promotes heterogeneous nucleation, thus increasing the degree of crystallinity.[19] It acts as a nucleating agent for the PP and changes the crystalline behavior of this polymer matrix.[20] As the clay content in the hybrid composite increases to 9 phr, (PP:G15)/NC9, the $X_c$ value is slightly reduced to 39.3%. This is probably so because this degree of crystallinity is very close to the maximum that the PP can achieve, considering its stereoregularity.[19] According to Fornes and Paul,[21] the presence of a high concentration of dispersed NC would prevent the formation of large crystalline domains, due to limited space and restrictions imposed on polymer chain by a high number of silicate platelets.

As for the crystalline peak temperature ($T_c$), no significant changes in $T_c$ values are observed with incorporation of GF and NC (PP/GF and PP/NC) to the system (Table 2, Figures 3 and 4). The same behavior has been observed when wood particles were incorporated into low-density polyethylene.[22] In contrast, the $T_c$ of the hybrid composites were enhanced to higher temperatures (Figure 4). The $T_c$ of the hybrids increase by about 3.8°C, 8.6°C, and 8.0°C, respectively, for the (PP:G15)/NC3, (PP:G15)/NC6, and (PP:G15)/NC9, relative to that of PP (121.7°C). These increments indicate the nucleating effect of the NC in the crystallization of PP.[4] Incorporation of NC and GF may accelerate the crystallization of PP, thereby making it to crystallize at higher temperature, hence shortening the molding cycle in practical production.[10] The same trend was observed for the enthalpy heat of crystallization, $\Delta H_c$.

## Dynamic mechanical analysis

*Storage modulus (E′).* The storage modulus ($E'$) is closely related to the load bearing capacity of a material and is analogous to the flexural modulus measured as per ASTM Standard D790.[2,23] Variation of $E'$ as a function of temperature for virgin PP, PP/GF, PP/NC, and PP/GF/NC composites is graphically illustrated in Figures 5(a) and 6(a). The thermomechanical data, as extracted from these curves, are tabulated in Table 3. From these figures, a decreasing trend in the storage modulus over the whole temperature range is observed. Two apparent changes in $E'$ with temperature can be observed for all the composites: a sharp rate of decrease in $E'$ from −25°C to about 25°C and a reduction in the rate of drop in $E'$ with temperature above 70°C. A significant fall in $E'$, in the region between −25°C and 25°C is believed to be associated with the relaxation of the amorphous phase ($\beta$-relaxation). In this case, the glassy state of the amorphous phase in the polymer matrix goes through its glass transition, followed by a sharp drop in $E'$. At about 15°C, the $E'$ continues to fall and the slope is flatter than what was obtained earlier in the first drop in $E'$. From 70°C and above, the reduction in $E'$ is less severe.

Figure 5(a) illustrates that the storage moduli of PP/NC composites show a dependence on the extent of NC loading below the glass transition temperature ($T_g$), while an insignificant variation of $E'$ between the composites is seen above the $T_g$. Generally, composites with higher NC loading (PP/NC6-9) possess higher moduli than the pure PP, through the whole temperature range. It is evident from Table 3 and Figure 5(a), that there is a notable increase in the modulus of PP/NC (at −100°C) with the incorporation of NC. This is probably due to the increase in the stiffness of the matrix

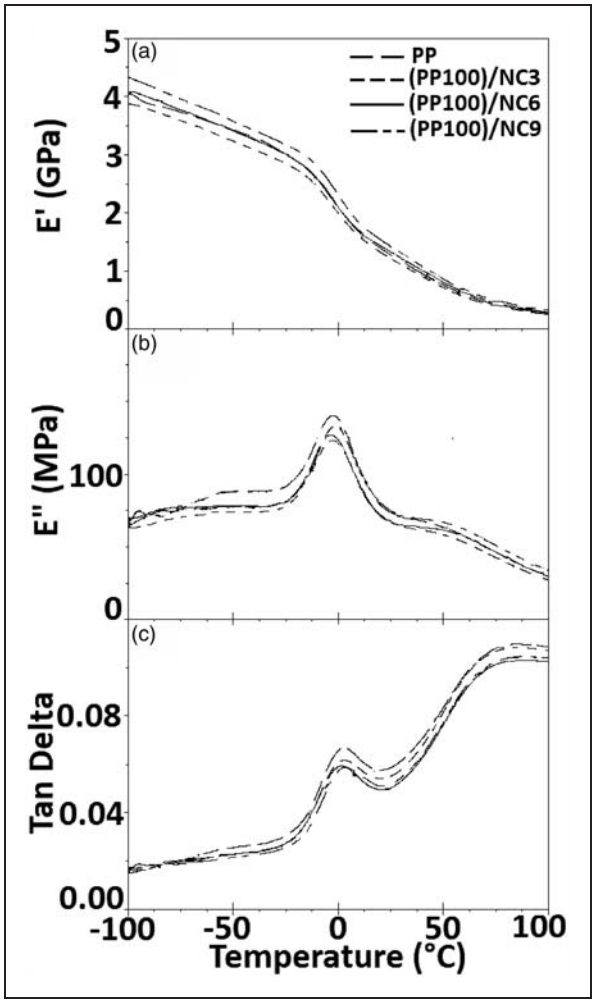


**Figure 5.** The DMA curves of injection-molded PP/NC composites.
DMA: dynamic mechanical analysis; PP: polypropylene; NC: nanoclay.

because of the restriction of molecular motions imparted by the NC.[24] The addition of 9 phr NC gives increment of about 6% in the storage modulus (at −100°C) relative to PP.

For the PP/G15 composite, incorporation of 15 wt% GF greatly increases the value of $E'$ at −100°C by about 56%, which is significantly higher compared with PP (Figure 6(a)). The incorporation of NC into PP/GF system further enhances this property. $E'$ of (PP/G15)/NC6 and (PP/G15)/NC9 composites (at −100°C) were increased by 63% and 73%, respectively, relative to PP, as NC was added to the PP/GF system. The improvement of $E'$ in the hybrid composites (PP/GF/NC) may be attributed, mainly due to the improvement of the matrix $E'$ from particulate filler dispersion. Thus, it seems that a synergistic effect did take place by incorporating particulate filler into the matrix, leading to a higher stiffness than would otherwise be expected,

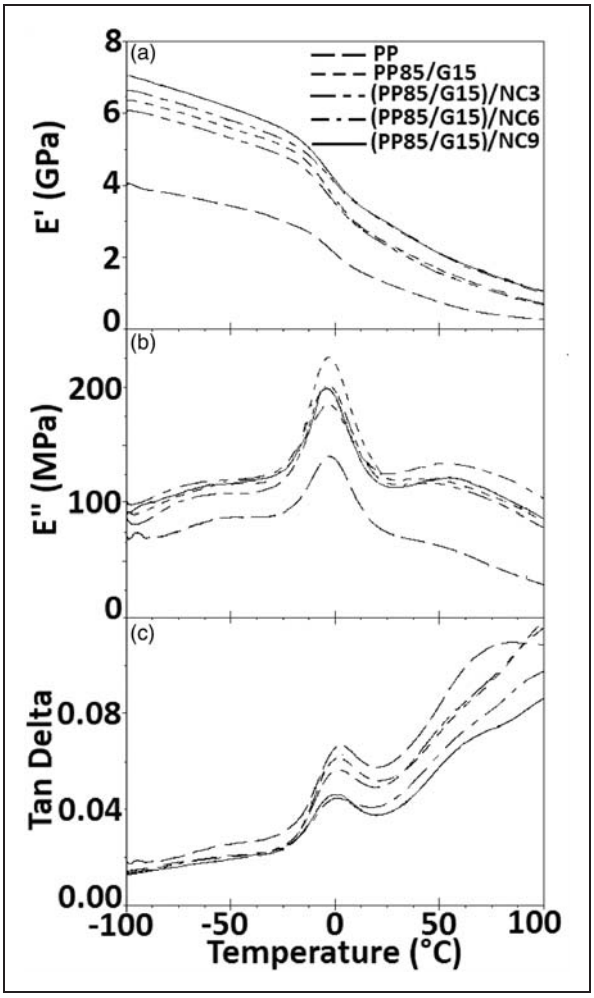


**Figure 6.** The DMA curves of injection-molded PP/GF/NC hybrid composites.
DMA: dynamic mechanical analysis; PP: polypropylene; GF: glass fiber; NC: nanoclay.

due solely to the change of the matrix modulus. In contrast, the (PP/G15)/NC3, registered a decrement in $E'$, relative to PP/G15 over the whole temperature range. Thus, it seems that the lower NC content gives negative effect as a filler.

*Loss modulus ($E''$).* The variations in $E''$ for the virgin PP, PP/NC, and PP/GF/NC hybrid composites as functions of temperature are shown in Figures 5(b) and 6(b). Samal et al.[18] reported that the PP exhibits three transition peaks ($\alpha$, $\beta$, and $\gamma$) at different temperatures within the investigated temperature range (−150°C to 150°C). The $\gamma$-transition at around −100°C is related to the relaxation of amorphous propylene segments of the PP chain. However, within the temperature range studied, the $\alpha$- and $\gamma$-transition peaks of the matrix polymer were not detected. The $\beta$-transition is due to the $T_g$ in the range of −10°C to 10°C and is associated with the motion of the long chain segments in the amorphous region of the PP. In this study, the $\beta$-transition peak of the matrix was observed at around −3°C.

In this study, $T_\beta^{E''}$ is referred to as the temperature at the maximum value of loss modulus in the $\beta$-transition region. As observed in Figures 5(b) and 6(b), PP/NC and PP/G15 composites show insignificant changes in the value, relative to the neat PP. By contrast, $T_\beta^{E''}$ of PP/GF/NC hybrid composites shifts to lower temperatures when compared with the PP. The decrease of $T_\beta^{E''}$ in this system indicates increased mobility of the amorphous part in the hybrids at lower temperature relative to neat PP.

*Loss tangent (tan $\delta$).* The ratio of the loss modulus to the storage modulus is measured as the mechanical loss or damping factor (tan $\delta$). The damping properties of the material give the balance between the elastic and

**Table 3.** DMA thermomechanical data of GF composites

| | Storage modulus, $E'$ (GPa) | | Loss modulus, $E''$ | | tan $\delta$ | |
|---|---|---|---|---|---|---|
| Sample | at −100°C | at 25°C | $E''_{max}$ (MPa) | $T_\beta^{E''}$ (°C) | tan $\delta_{max}$ ($\times 10^{-2}$) | $T_g$ (°C) |
| PP | 4.1 | 1.28 | 140 | −3 | 6.7 | 3 |
| (PP100)/NC3 | 3.9 | 1.21 | 123 | −3 | 6.2 | 2 |
| (PP100)/NC6 | 4.1 | 1.33 | 127 | −4 | 5.9 | 2 |
| (PP100)/NC9 | 4.3 | 1.42 | 133 | −1 | 5.9 | 3 |
| (PP85:G15) | 6.4 | 2.39 | 226 | −3 | 6.2 | 2 |
| (PP85:G15)/NC3 | 6.1 | 2.32 | 202 | −4 | 5.6 | 1 |
| (PP85:G15)/NC6 | 6.7 | 2.93 | 185 | −3 | 4.5 | 1 |
| (PP85:G15)/NC9 | 7.1 | 2.98 | 199 | −5 | 4.6 | −1 |

DMA: dynamic mechanical analysis; PP: polypropylene; NC: nanoclay.

viscous phase in a polymeric structure.[2] The variations of tan $\delta$ as a function of temperature are represented in Figures 5(c) and 6(c). The transition region as indicated by damping maxima is usually known as the β-transition.

By analyzing the tan $\delta$ curves for PP/GF, PP/NC, and PP/GF/NC composites, no significant difference in $T_g$ value can be observed. The same trend has been reported by Modesti et al.[19] It is suggested, therefore, that the $T_g$ is not significantly affected by the presence of GF and NC. However, the presence of the GF and NC reduces the magnitude of tan $\delta_{max}$ values. Higher reduction for composite with higher filler loading is believed to be due to the strengthening effect of the GF and NC, thus limiting the mobility of the polymer matrix. In this case, the incorporation of GF and NC which act as barriers to the mobility of polymer chain, leads to a lower degree of molecular motion and consequently lowering damping characteristics.[25] Another possible reason is that there is less matrix, by volume, to dissipate the vibration energy. Incorporation of NC in PP/GF composite further reduces this value. The tan $\delta_{max}$ for (PP/G15)/NC6 shows a maximum decrease of about 32% (from 0.0667 to 0.0450) when compared with the pure matrix. A decline in the tan $\delta$ values with the addition of NC, indicates an improvement in the interfacial adhesion of the composites.[26]

## Impact properties

Generally, the resistance to crack propagation or fracture toughness of the PP/NC and PP/GF/NC composites is characterized by measuring the $G_c$ (critical strain energy release rate) and $K_c$ (stress intensity factor), using SEN specimens in a 3-PB set-up,[15] according to ASTM standard E23. Both parameters can be taken as measures of the interfacial strength. Linear elastic fracture mechanics methodologies have been used to characterize the toughness of composites and plastics in terms of $G_c$ or $K_c$ of polymeric materials. They have been found to be effective approaches to characterize brittle polymers.

The relationship[27,28] between $W$, $G_c$, and specimen geometry parameter ($BD\Phi$) is given by

$$W = G_c BD\Phi \tag{2}$$

where $B$ and $D$ are the width and depth of the specimen, respectively. A correction factor, $\Phi$ is given by

$$\Phi = \frac{1}{2}\left(\frac{a}{D}\right) + \frac{1}{18\pi}\left(\frac{S}{D}\right)\left(\frac{a}{D}\right)^{-1} \tag{3}$$

where $a$ and $S$ are the notch depth (or crack length) and span of the specimens, respectively.

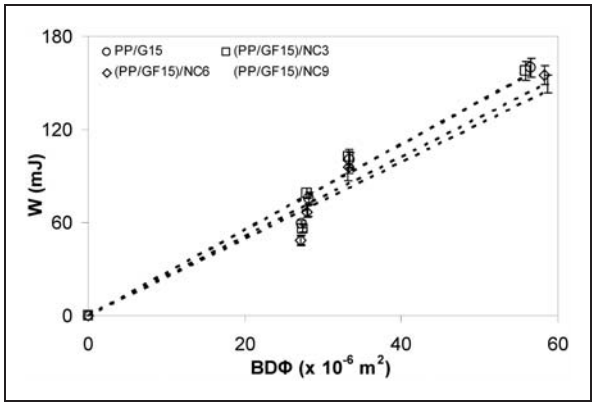


**Figure 7.** Plot of $W$ as a function of $BD\Phi$ of the PP/GF/NC hybrid composites.
PP: polypropylene; GF: glass fiber; NC: nanoclay.

On a plot of $W$ against $BD\Phi$ (Figure 7), a straight line is obtained through the origin and its slope is taken as the $G_c$ of the materials. The relationship between the $K_c$ with nominal fracture stress ($\sigma$), geometry correction factor ($Y$), and notch or crack length ($a$) is given by

$$\sigma Y = \frac{K_c}{\sqrt{a}} \tag{4}$$

In a 3-PB test, $\sigma$ is given by the simple bending theory as

$$\sigma = \frac{6PS}{4BD^2} \tag{5}$$

For the 3-PB test specimen, where $S/D$ is equal to 4, $Y$ is given by

$$Y = 1.93 - 3.07\left(\frac{a}{D}\right) + 14.53\left(\frac{a}{D}\right)^2 - 25.11\left(\frac{a}{D}\right)^3 + 25.80\left(\frac{a}{D}\right)^4 \tag{6}$$

On a plot of $\sigma Y$ against $a^{-0.5}$ (Figure 8), a straight line is obtained through the origin and its slope is taken as the $K_c$ of the materials. Details of this method have been explained by Karger-Kocsis[29] and Hassan et al.[27] Similar plots are also obtained for PP/NC composites. The $G_c$ and $K_c$ values for these composites, as extracted from the plots, are shown in Figure 9. The PP matrix has a $G_c$ value of 4.4 kJ/m$^2$, which is 83% higher than those calculated by Karger-Kocsis[29] (2.4 kJ/m$^2$) by instrumented high-speed impact bending test. The difference between the two values could be due to material grade, processing method (compression or injection molding), testing mode (charpy or izod), etc.

There is a sharp decrease in $G_c$ (32%) with the initial incorporation of 3 phr NC loading, when compared

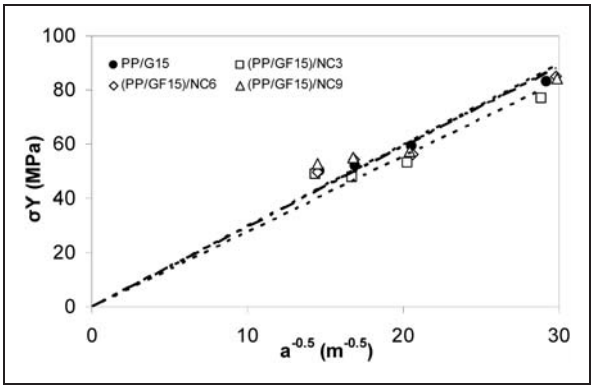


**Figure 8.** Plot of $\sigma Y$ as a function of $a^{-0.5}$ of the PP/GF/NC hybrid composites.
PP: polypropylene; GF: glass fiber; NC: nanoclay.

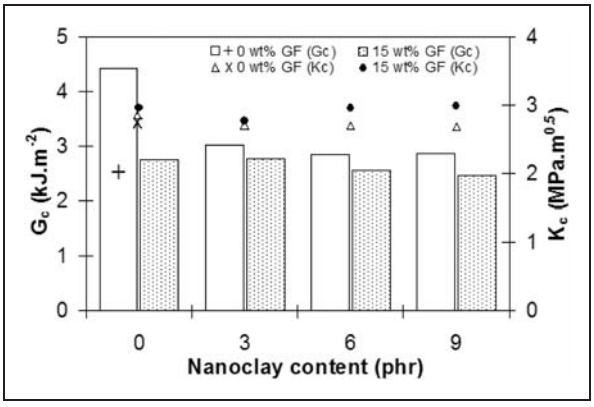


**Figure 9.** $G_c$ and $K_c$ of PP/NC and PP/GF/NC hybrid composites. Designation: values given by symbols + and × were taken from the work of Karger-Kocsis.[29]
PP: polypropylene; GF: glass fiber; NC: nanoclay.

with the PP matrix. It is interesting to note that further addition of NC, to 6 and 9 phr, does not produce any significant effect on the impact strength. For the hybrid composites, incorporation of NC into the PP/GF15 system further reduces the $G_c$, as the higher NC loading results in a lower $G_c$ value. There is about 44% reduction in the $G_c$ value observed, with the incorporation of 9 phr NC into PP/GF15, relative to PP matrix. The reduction in $G_c$ with NC concentration implies that the hybrid composites systems have became more brittle when compared with the neat PP matrix. Chow et al.[30] suggested that the agglomeration of NC may induce local stress concentration, thus the nanocomposite fails, in a more brittle manner. Li et al.[31] also reported that any polymer nanocomposites will show an increase in tensile strength and modulus with simultaneous loss in the $G_c$. Lower $G_c$ at high NC content can possibly be attributed to the agglomeration of NC in the nanocomposite system. $K_c$ value of 2.9 MPa/m$^{0.5}$ is obtained for the PP matrix. This is comparable with that reported by Karger-Kocsis[29] (2.8 MPa/m$^{0.5}$). Although the $G_c$ values are affected by test fixture,[27] $K_c$ seems to be independent of the specimen geometry. Addition of NC into PP matrix and PP/GF composites does not result in any significant effect on the $K_c$ values (Figure 9).

## Conclusions

Introducing the NC in the PP matrix, resulted in no significant changes on the melting temperature of the composite, but for the hybrid composites, the values seemed to increased. The enthalpy heat of melting values for PP/NC nanocomposites were lowered when compared with neat PP. For the hybrid systems, it was observed that the enthalpy heat of melting and the degree of crystallinity values of composites, generally increased with increasing clay content. The enthalpy heat of crystalline and the crystallization temperature value of the hybrid composites are enhanced to higher degrees when compared with the conventional PP/GF and PP/NC composites.

Generally, composites with higher NC loading possessed higher storage modulus than the neat PP matrix, over the whole temperature range studied. The temperature at the maximum value of loss modulus in the $\beta$-transition region shifted to a lower temperature and its magnitude was reduced when compared with the neat PP. Incorporation of NC and GF reduced the magnitude of $\tan \delta_{max}$ values.

A decrease in critical strain energy release rate with incorporation of NC into the PP/GF15 was observed. Addition of NC into PP matrix and PP/GF composites does not result in any significant effect on the stress intensity factor values.

### Funding

This work was funded by the University of Malaya under (grant nos. PPP (PS230/2008B, PS376/2009B, and PS504/2010B)).

### References

1. Seo MK, Lee JR and Park SJ. Crystallization kinetics and interfacial behaviors of polypropylene composites reinforced with multi-walled carbon nanotubes. *Mater Sci Eng A* 2005; 404(1–2): 79–84.
2. Hassan A, Normasmira AR and Yahya R. Extrusion and injection-molding of glass fiber/MAPP/polypropylene: effect of coupling agent on DSC, DMA and mechanical properties. *J Reinf Plast Compos* 2011; 30(14): 1223–1232.
3. Karger-Kocsis J. Dependence of the fracture and fatigue performance of polyolefins and related blends and

composites on microstructural and molecular characteristics. *Macromol Symp* 1999; 143: 185–205.
4. Lei SG, Hoa SV and Ton-That MT. Effect of clay types on the processing and properties of polypropylene nanocomposites. *Compos Sci Technol* 2006; 66(10): 1274–1279.
5. Hartikainen J, Hine P, Szabó JS, et al. Polypropylene hybrid composites reinforced with long glass fibres and particulate filler. *Compos Sci Technol* 2005; 65(2): 257–267.
6. Mohan TP and Kanny K. Influence of nanoclay on rheological and mechanical properties of short glass fiber-reinforced polypropylene composites. *J Reinf Plast Compos* 2011; 30(2): 152–160.
7. Kornmann X, Rees M, Thomann Y, et al. Epoxy-layered silicate nanocomposites as matrix in glass fibre-reinforced composites. *Compos Sci Technol* 2005; 65(14): 2259–2268.
8. Normasmira AR, Hassan A, Yahya R, et al. Micro-structural, thermal and mechanical properties of injection-molded glass-fiber/nanoclay/polypropylene composites. *J Reinf Plast Compos* 2012; 31(4): 269–281.
9. Vlasveld DPN, Bersee HEN and Picken SJ. Nanocomposite matrix for increased fibre composite strength. *Polymer* 2005; 46(23): 10269–10278.
10. Cui YH, Wang XX, Li ZQ, et al. Fabrication and properties of nano ZnO/glass fiber reinforced polypropylene composites. *J Vinyl Add Techn* 2010; 16(3): 189–194.
11. Acosta JL, Rocha CM, Ojeda MC, et al. The effect of several modified sepiolites on the transition temperatures and crystallinity of filled propylene. *Angew Makromol Chem* 1984; 126: 51–57.
12. Wright DGM, Dunk R, Bouvart D, et al. The effect of crystallinity on the properties of injection moulded polypropylene and polyacetal. *Polymer* 1988; 29(5): 793–796.
13. Jordan J, Jacob KI, Tannenbaum R, et al. Experimental trends in polymer nanocomposites – a review. *Mater Sci Eng A* 2005; 393(1–2): 1–11.
14. ASTM Standard D-638:2003. Standard test method for tensile properties of plastics. West Coshoshocken, PA: ASTM International. DOI 10.1520/D0638-03, www.astm.org.
15. ASTM Standard E23-07ae1:2007. Standard test method for notched bar impact testing of metallic materials. West Coshoshocken, PA: ASTM International. www.astm.org.
16. Hussain F, Roy S, Narasimhan K, et al. E-glass – polypropylene pultruded nanocomposite: manufacture, characterization, thermal and mechanical properties. *J Thermoplast Compos Mater* 2007; 20(4): 411–434.
17. Sichina WJ. *Prediction of end-use characteristics of polyethylene materials using differential scanning calorimetry*. USA: Application Briff DSC-11. Shelton, CT: Perkin Elmer Instruments LLC, 1994.
18. Samal SK, Mohanty S and Nayak SK. Polypropylene—bamboo/glass fiber hybrid composites: fabrication and analysis of mechanical, morphological, thermal, and dynamic mechanical behavior. *J Reinf Plast Compos* 2009; 28(22): 2729–2747.
19. Modesti M, Lorenzetti A, Bon D, et al. Thermal behaviour of compatibilised polypropylene nanocomposite: effect of processing conditions. *Polym Degrad Stab* 2006; 91(4): 672–680.
20. Kulshreshtha AK, Maiti AK, Choudhary MS, et al. Nano addition of raw bentonite enhances polypropylene (PP) properties. *J Appl Polym Sci* 2006; 99(3): 1004–1009.
21. Fornes TD and Paul DR. Crystallization behavior of nylon 6 nanocomposites. *Polymer* 2003; 44(14): 3945–3961.
22. Lafia-Araga RA, Hassan A, Yahya R, et al. Thermal and mechanical properties of treated and untreated Red Balau (Shorea dipterocarpaceae)/LDPE composites. *J Reinf Plast Compos* 2012; 31(4): 215–224.
23. Saha AK, Das S, Bhatta D, et al. Study of jute fiber reinforced polyester composites by dynamic mechanical analysis. *J Appl Polym Sci* 1999; 71(9): 1505–1513.
24. Bozkurt E, Kaya E and Tanoglu M. Mechanical and thermal behavior of non-crimp glass fiber reinforced layered clay/epoxy nanocomposites. *Compos Sci Technol* 2007; 67(15–16): 3394–3403.
25. López-Manchado MA, Biagiotti J and Kenny JM. Comparative study of the effects of different fibers on the processing and properties of polypropylene matrix composites. *J Thermoplast Compos Mater* 2002; 15(4): 337–353.
26. Nayak SK and Mohanty S. Sisal glass fiber reinforced PP hybrid composites: effect of MAPP on the dynamic mechanical and thermal properties. *J Reinf Plast Compos* 2010; 29(10): 1551–1568.
27. Hassan A, Hassan AA and Mohd Rafiq MI. Impact properties of injection molded glass fiber/polyamide-6 composites: effect of testing parameters. *J Reinf Plast Compos* 2011; 30(10): 889–898.
28. Hassan A, Hornsby PR and Folkes MJ. Structure-property relationship of injection moulded carbon fibre reinforced polyamide 6,6 composites: the effect of compounding routes. *Polym Test* 2003; 22(2): 185–189.
29. Karger-Kocsis J. Instrumented impact fracture and related behavior in short- and long-glass-fiber-reinforced polypropylene. *Compos Sci Technol* 1993; 48: 273–283.
30. Chow WS, Mohd Ishak ZA, Karger-Kocsis J, et al. Compatibilizing effect of maleated polypropylene on the mechanical properties and morphology of injection molded polyamide 6/polypropylene/organoclay nanocomposites. *Polymer* 2003; 44(24): 7427–7440.
31. Li X, Park HM, Lee JO, et al. Effect of blending sequence on the microstructure and properties of PBT/EVA g MAH/organoclay ternary nanocomposites. *Polym Eng Sci* 2002; 42(11): 2156–2164.